NON-VASCULAR INTERVENTIONAL PROCEDURES: EFFECTIVE DOSE TO PATIENT AND EQUIVALENT DOSE TO ABDOMINAL ORGANS BY MEANS OF DICOM IMAGES AND MONTE CARLO SIMULATION

ARTICLE *in* RADIATION PROTECTION DOSIMETRY · JULY 2015

Impact Factor: 0.91 · DOI: 10.1093/rpd/ncv362 · Source: PubMed

10 AUTHORS, INCLUDING:

Fabrizio Fanelli
Sapienza University of Rome
122 PUBLICATIONS **1,202** CITATIONS
SEE PROFILE

Elisabetta di castro
Sapienza University of Rome
26 PUBLICATIONS **99** CITATIONS
SEE PROFILE

Radiation Protection Dosimetry (2015), pp. 1–7 doi:10.1093/rpd/ncv362

NON-VASCULAR INTERVENTIONAL PROCEDURES: EFFECTIVE DOSE TO PATIENT AND EQUIVALENT DOSE TO ABDOMINAL ORGANS BY MEANS OF DICOM IMAGES AND MONTE CARLO SIMULATION

Mariaconcetta Longo[1,*], Chiara Marchioni[1], Teresa Insero[1], Raffaella Donnarumma[1], Alessandro D'Adamo[2], Pierleone Lucatelli[2], Fabrizio Fanelli[2], Filippo Maria Salvatori[2], Alessandro Cannavale[2] and Elisabetta Di Castro[3]
[1]Post Graduate School of Medical Physics, Sapienza University of Rome, Rome, Italy
[2]Department of Radiological Sciences, Vascular and Interventional Unit, Sapienza University of Rome, Rome, Italy
[3]Department of Radiological Sciences, Health Physic Unit, Sapienza University of Rome, Rome, Italy

*Corresponding author: longo.mariaconcetta@gmail.com

Received 15 April 2015; accepted 10 June 2015

This study evaluates X-ray exposure in patient undergoing abdominal extra-vascular interventional procedures by means of Digital Imaging and COmmunications in Medicine (DICOM) image headers and Monte Carlo simulation. The main aim was to assess the effective and equivalent doses, under the hypothesis of their correlation with the dose area product (DAP) measured during each examination. This allows to collect dosimetric information about each patient and to evaluate associated risks without resorting to *in vivo* dosimetry. The dose calculation was performed in 79 procedures through the Monte Carlo simulator PCXMC (A PC-based Monte Carlo program for calculating patient doses in medical X-ray examinations), by using the real geometrical and dosimetric irradiation conditions, automatically extracted from DICOM headers. The DAP measurements were also validated by using thermoluminescent dosimeters on an anthropomorphic phantom. The expected linear correlation between effective doses and DAP was confirmed with an R^2 of 0.974. Moreover, in order to easily calculate patient doses, conversion coefficients that relate equivalent doses to measurable quantities, such as DAP, were obtained.

INTRODUCTION

Over the past decade, expansion of the X-ray imaging has been dramatic, especially for computed tomography (CT), angiography and interventional procedures that give the largest contribution to the total collective dose from all X-ray examinations.

In particular, interventional radiology (IR) procedures are profoundly different from diagnostic radiology exams due to their therapeutic purpose, which can shift the risk–benefit ratio for radiation exposure[(1)]. Therefore, there is a significant concern related to the risk of radiation-induced cancer in patients undergoing fluoroscopically guided interventional procedures[(2)].

In radiation protection and radiology, effective dose (E) and equivalent dose (H_T) still provide a good evaluation of the cancer risk to a whole or part of organism due to ionising radiation delivered non-uniformly to the part(s) of its body[(3)]. Indeed, patient dose report is currently considered the main tool for the medical physicists to optimise the dose released during IR procedures according to the clinical aim.

Differently from other examinations, interventional procedures may have high variability according to the type of X-ray equipment, the body region and the kind and complexity of intervention. In particular, non-vascular procedures may be repeated and may need multiple fluoroscopy controls, also over a long-time follow-up. As exposure conditions vary considerably throughout a single procedure and X-rays exposure could be prolonged, a patient-specific dosimetry is both necessary and difficult[(4)]. Furthermore, dosimetric assessment is mandatory as recommended by the Council Directive 2013/59/EURATOM, which lays down basic safety standards for protection against the dangers arising from exposure to ionising radiation.

The dose delivered to a patient during an interventional procedure can be evaluated a posteriori by using several methods. On one side, entrance surface dose (ESD) may be measured by using Gafchromic films and thermo-luminescent dosemeters (TLDs) placed on the surface of a patient or a phantom (simulating the part of an average patient under examination). On the other side, Monte Carlo simulations applied on mathematical phantoms have been developed to evaluate E and H_T by modelling the energy deposition in the human body.

Many studies evaluated the ESD and its relation with skin injuries and adverse tissues reactions, which are related to deterministic effects, for both vascular and non-vascular interventional procedures[(5–7)]. In particular, the complexity of non-vascular procedures

and the related high exposure times led to investigate the associated radiation exposure. Kloeckner et al.[8] analysed the overall radiation dose released during non-vascular interventions as biliary procedures, embolisations and percutaneous collection drainages. Karavasilis et al.[9] and Stratakis et al.[10] reported equivalent organs doses associated to biliary drainage procedures; according to the latter, the organs receiving the higher amount of radiations doses were the lumbar spine, kidneys and adrenals.

Despite of these studies, the effective dose and the abdominal organs equivalent doses have not yet well investigated for some other classes of non-vascular abdominal procedures. The main aim of the present study was to estimate patient-specific radiation doses in a group of abdominal extra-vascular interventions using geometric and dosimetric irradiation data automatically extracted from the DICOM header of each examination. Moreover, coefficients to convert dose area product (DAP) to equivalent doses and effective doses were evaluated in order to easily relate the dosimetric quantities E and H_T to a measurable quantity.

MATERIALS AND METHODS

In the current study, a total of 49 patients who underwent 79 non-vascular interventional procedures in an IR institution were included and analysed. This study met the criteria of the Declaration of Helsinki and was carried out with the informed consent of all patients. The selected procedures were urinary system interventions (unilateral, bilateral nephrostomy, fluoroscopic control of nephrostomy, urinary stents management), liver/biliary interventions [percutaneous cholangiography (PTC), unilateral or bilateral biliary drainage placement, biliary stent placement, cholecystectomy, fluoroscopic controls of those procedures], drainage of abscess, fluid collections and subsequent fluoroscopic controls. These procedures represent the clinical routine in the institution and were performed by three experienced interventional radiologists (with 4, 15 and 30 years of experience, respectively). The studied interventions were divided into categories according to the type of intervention (urinary procedures, biliary procedures and collection drainages), Table 1, and to the abdominal region involved (epigastric region and adjacent ones, umbilical region and adjacent ones, hypogastric region and adjacent ones), Table 2.

This separation into categories was necessary to identify the main organs at risk based on the type of intervention and the region involved.

The X-ray imaging system used in this study was the Angiographer Siemens Artis Zee (Siemens, Erlangen, Germany) with a large-area (30×40 cm^2) flat-panel Si detector with CsI as scintillation material. An inherent filtration of 2.5 mmAl and a tube voltage ranged from 71 to 81 kVp, through automatic exposure control,

Table 1. Patient data for each intervention.

	Urinary	Biliary	Drainage of collections
Number of procedures	14	22	43
Patient number	7	16	26
Gender (M:F)	5:2	11:5	13:13
Age, y[a]	60.4 ± 5.4	65.0 ± 6.9	60.8 ± 11.5
Height, cm[a]	173.5 ± 5.0	172.8 ± 5.5	167.8 ± 8.5
Weight, kg[a]	82.2 ± 10.4	72.0 ± 8.3	67.1 ± 12.4
BMI, kg m^{-2}[a]	27.4 ± 3.9	24.0 ± 2.6	24.0 ± 3.2

[a]Mean $\pm$ SD.

Table 2. Patient data for each district.

	Epigastric region and adjacent	Umbilical region and adjacent	Hypogastric region and adjacent
Number of procedures	31	24	24
Patient number	23	19	17
Gender (M:F)	16:7	13:6	8:9
Age, y[a]	69.4 ± 9.8	60.0 ± 7.1	60.8 ± 11.6
Height, cm[a]	171.0 ± 7.2	171.4 ± 5.3	169.6 ± 9.3
Weight, kg[a]	69.4 ± 9.8	75.3 ± 11.7	73.6 ± 16.1
BMI, kg m^{-2}[a]	23.8 ± 2.3	25.9 ± 4.0	25.9 ± 4.4

[a]Mean $\pm$ SD.

were used. Both radiography and fluoroscopy (10 pulses per second with a pulse width of 15 ms) were recorded, while the field size varied with the collimators position. For all procedures, the same low-radiation-exposure protocol was used in order to guarantee a standard for all X-ray examinations.

According to the recent European guidelines, all newly installed radiological devices have to provide an indication of patient dose. In digital X-ray equipment, this indication could be given in terms of DAP or entrance air kerma (EAK), which are automatically stored in the DICOM header image files or in a system report file. In order to provide a DAP indication, the used angiographer is equipped with a calibrated air ionisation chamber DAP meter, incorporated in the tube housing. The system provides a readout of the cumulative DAP for every image run and the EAK, which is calculated from the measured DAP at a specific point, called intervention reference point (IRP) and located at 63.5 cm from the X-ray source.

To ensure that the system was properly calibrated, i.e. the DAP and EAK values provided by the device were accurate, a set of experimental measurements were previously performed. The angiographer ionisation chamber accuracy was verified using an external calibrated DAP meter (DAP/dose meter KermaX plus TinO IDP), while the correctness of the EAK provided by the angiographic system was validated by performing ESD measurements with TLDs on the Anderson-Rando anthropomorphic phantom. For this purpose, TLDs (LiF100) were applied on the prone phantom abdomen at the centre of the radiation field (Figure 1).

The TLDs were irradiated at different exposures levels, varying the exposure time (6, 8, 10 and 12 min) with an X-ray field of 25 × 25 cm^2 at 70 kVp; these dosemeters measured the personal dose equivalent H_p (0.07). The ESD values resulting from TLD reading were compared with the ESD calculated from the EAK provided by the system report file. As the angiographer provides the EAK at the IRP without the backscatter contribution, the following correction has to be applied:

$$\mathrm{ESD} = \mathrm{EAK_{IRP}} \times \mathrm{BSF} \times \left(\frac{\mathrm{SSD}}{\mathrm{SRD}}\right)^2, \qquad (1)$$

where SSD and SRD represent the source-to-surface and the source-to-reference point distances, respectively, while BSF is the backscatter factor that arises from the radiation backscattered from the phantom. Equation 1 allows to scale the EAK at the plane where TLD is placed, and it is valid under conditions of electron equilibrium, which can be assumed to apply to low-energy and medium-energy X-ray beams at the depth 0.07 mm, i.e. the measuring depth of the personal dose equivalent H_p (0.07).

An automated method to extract patient (weight and height), exposure, geometric and dosimetric (DAP or EAK) parameters from the headers of DICOM image files was developed in the MATLAB (MathWorks, Natick, MA) environment and applied to the sets of the present study examinations. These extracted data were then used as input for the Monte Carlo simulator PCXMC (STUK, Finland, Servomaa and Tapiovaara 1998).

This program allows a free adjustment of the X-ray beam direction and other examination conditions of projection in radiographic and fluoroscopic irradiation. Parameters such as X-ray tube voltage (kVp), total beam filtration, focus to skin distance (FSD), degrees rotation around the patient's longitudinal axis and in craniocaudal direction, skin entry point of the central beam axis (in terms of coordinates x_{ref}, y_{ref} and z_{ref}) and field size (A_{skin}) at this position had to be provided. These parameters allowed simulating the real

Figure 1. Experimental validation setting.

irradiation conditions of patients during each procedure. In order to calculate the effective and the equivalent doses, the program uses the DAP (in mGy cm^2) value or alternatively the EAK, in mGy and without backscatter, reported in the DICOM header of image files. The developed MATLAB software allows to automatically extract all the mentioned data from the DICOM headers of each examination. In particular, X-ray tube voltage (kVp), total beam filtration, FSD, and degrees of rotation about the main axis were directly extracted from DICOM tags, while the field size A_{skin} was calculated by the software using collimator positions and imager pixel size extracted from respective tags[11]:

$$A_{\text{skin}} = \left[(|C_L - C_R| \times \left(\frac{p}{10}\right) \times (|C_T - C_B| \times \left(\frac{p}{10}\right) \right] \times \left(\frac{\text{SPD}}{\text{SID}}\right), \quad (2)$$

where C_L, C_R, C_T and C_B are the collimator positions in pixels in left, right, top and bottom, respectively, and p is the imager pixel size in mm. SPD and SID represent the source-to-patient and the source-to-image distances, respectively.

Moreover, in order to identify the organs really covered by the irradiation field, it is necessary to identify the central location of the field. As a matter of fact, as the skin entry point of the central beam axis depends on the irradiation conditions (patient position, orientation of the C arm), the coordinates x_{ref}, y_{ref} and z_{ref} were identified according to division of the abdomen into nine regions. The coordinates x_{ref} and z_{ref} corresponded to the centres of these regions, thus ensuring a better dose evaluation for the organs covered by the X-ray field. A linear regression analysis was performed to explore the correlations between DAP and effective doses or equivalent doses to abdominal organs. For all fitting procedures, the correlation coefficients R^2 were calculated in order to take into account the goodness of fits.

RESULTS

Firstly, the validation of DAP and EAK provided by the angiographer is discussed. The DAP values, measured and provided by the angiographer, agree within the expected range of values. Moreover, the comparison between the ESDs, measured (by TLD dosemeters) and calculated using the EAK extracted from the system report file, is in agreement (Figure 2) within the reported overall uncertainty of the TLD method.

Secondly, equivalent doses for the organs included in the radiation field were evaluated according to the involved region (epigastric region and adjacent ones, umbilical region and adjacent ones, hypogastric region and adjacent ones). A linear fit of the equivalent doses as function of DAP was performed for such districts. Table 3 presents the DAP range, the results of simulation (equivalent dose range, its mean value and standard error) and the results of statistical analysis (conversion coefficients C between DAP and equivalent doses for abdominal organs, in mSv Gy^{-1} cm^{-2}, and the resulting R^2).

This analysis shows that it is possible to deduce H_T from DAP by using the appropriate conversion coefficients, although somewhere with a weaker correlation. As it can be seen in Table 3, for the procedures performed at the level of the upper quadrants (epigastric regions and adjacent zones), the organs mostly exposed to radiations were the kidneys (mean equivalent dose $\overline{H_T}$ of 41.7 mSv), gallbladder ($\overline{H_T}$ of 7.5 mSv) and adrenals ($\overline{H_T}$ of 7.1 mSv). In the mid-quadrants, higher equivalent doses were delivered to the small intestine ($\overline{H_T}$ of 9.6 mSv), active bone marrow ($\overline{H_T}$ of 9.2 mSv), kidneys ($\overline{H_T}$ of 5.6 mSv) and colon ($\overline{H_T}$ of 5.1 mSv). In the lower quadrants, higher radiation doses were delivered to the urinary bladder ($\overline{H_T}$ of 5.0 mSv), colon ($\overline{H_T}$ of 3.7 mSv) and active bone marrow ($\overline{H_T}$ of 3.7 mSv).

Moreover, the mean equivalent doses were investigated for the three subgroups that represent the different type of interventions. The calculated mean equivalent dose values related to the organs receiving considerable amounts of radiation doses, for urinary procedures, biliary procedures and collection drainages, respectively, are presented through the histogram of Figure 3.

Furthermore, as expected, the study confirmed a linear correlation between DAP (device output reported on DICOM tags) and effective dose (simulation output), Figure 4, with an R^2 of 0.974. The linear fit of E as function of DAP resulted in a conversion coefficient of 0.089 ± 0.009 mSv Gy^{-1} cm^{-2}. This conversion coefficient allows to directly evaluate E from the DAP, provided in the system report file, without resorting to *in vivo* dosimetry.

DISCUSSION

The presented method allowed defining and analysing the X-ray dose released to patients undergoing extravascular examinations without resorting to *in vivo* dosimetry. Monte Carlo simulation (PCXMC code) was used in conjunction with DAP measurements in order to estimate both H_T and E for each examination. The confirmed linear correlation between DAP and effective dose represents an important tool to directly deduce E from DAP for each patient. Nowadays, the recommended dose levels are referred to DAP value, which is the most common measureable dose indicator[12–14]. The UK National Patient Dose Database (NPDD) provided the latest set of European reference doses for eight interventional procedures, in terms of both total DAP and total fluoroscopy time[15]. Also other authors proposed reference levels for some non-vascular interventional procedures (biliary drainages, nephrostomies)[16].

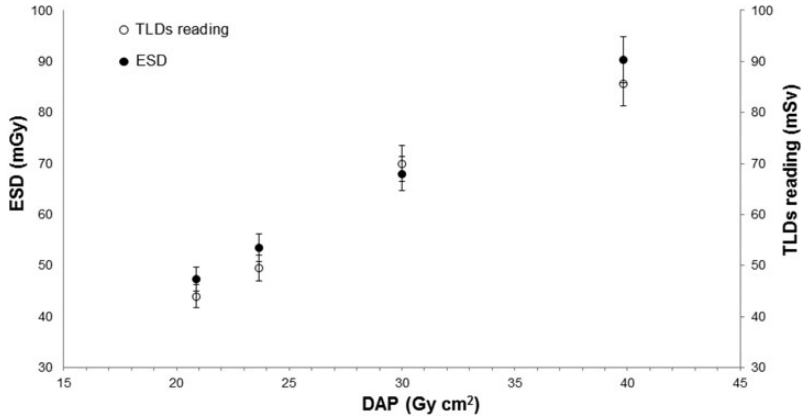

Figure 2. Comparison between TLD and ESD values.

Table 3. DAP range, results of simulation and statistical analysis for each district.

	DAP range (Gy cm^2)		H_T range (mSv)	$\overline{H_T}$ (mSv)[a]	C (mSv Gy^{-1} cm^{-2})	R^2
Epigastric region and adjacent ones	1.75–76.25	Active bone marrow	0.15–13.92	3.01 ± 0.13	0.123	0.750
		Adrenals	0.38–42.73	7.07 ± 0.30	0.275	0.675
		Colon	0.16–10.19	3.18 ± 0.11	0.123	0.966
		Gall bladder	0.17–35.90	7.47 ± 0.31	0.297	0.766
		Kidneys	1.47–150.10	41.73 ± 1.59	1.653	0.897
		Liver	0.06–32.57	6.29 ± 0.30	0.237	0.483
		Pancreas	0.17–22.31	5.23 ± 0.22	0.275	0.675
		Skin	0.12–6.84	2.37 ± 0.08	0.090	0.991
		Small intestine	0.26–19.10	5.04 ± 0.18	0.196	0.933
		Spleen	0.02–59.71	7.31 ± 0.44	0.226	0.103
		Stomach	0.03–15.22	3.04 ± 0.15	0.109	0.370
Umbilical region and adjacent ones	1.78–249.06	Active bone marrow	0.29–87.93	9.22 ± 0.76	0.327	0.977
		Colon	0.19–38.32	5.04 ± 0.37	0.152	0.957
		Gall bladder	0.06–6.94	1.98 ± 0.09	0.039	0.420
		Kidneys	0.34–26.03	5.60 ± 0.31	0.121	0.428
		Skin	0.14–29.36	3.33 ± 0.26	0.115	0.989
		Small intestine	0.32–75.11	9.63 ± 0.66	0.298	0.978
Hypogastric region and adjacent ones	1.48–198.20	Active bone marrow	0.13–34.46	3.72 ± 0.30	0.710	0.994
		Colon	0.06–39.14	3.74 ± 0.33	0.187	0.981
		Skin	0.09–24.91	2.38 ± 0.21	0.018	0.981
		Small intestine	0.06–17.00	2.06 ± 0.15	0.088	0.989
		Urinary bladder	0.14–40.02	4.93 ± 0.37	0.213	0.965

[a]Organ equivalent doses are expressed in term of mean value and standard error.

According to these references, biliary interventions have the highest reference dose (50 Gy cm^2) of all procedures. Otherwise, the DAP-recommended limit for nephrostomies is 14 Gy cm^2, while the limits for drainages of collection are not provided. The biliary procedures studied in this article had overcome the recommended threshold in the 20 % of cases. For urinary interventions (unilateral, bilateral nephrostomy, fluoroscopic control of nephrostomy, urinary stents management), it is not possible to provide a similar comparison, because the recommended limit is provided for nephrostomies only.

The main advantages of the proposed method lie in the possibility to take into account the high variability of the studied procedures, as it uses for

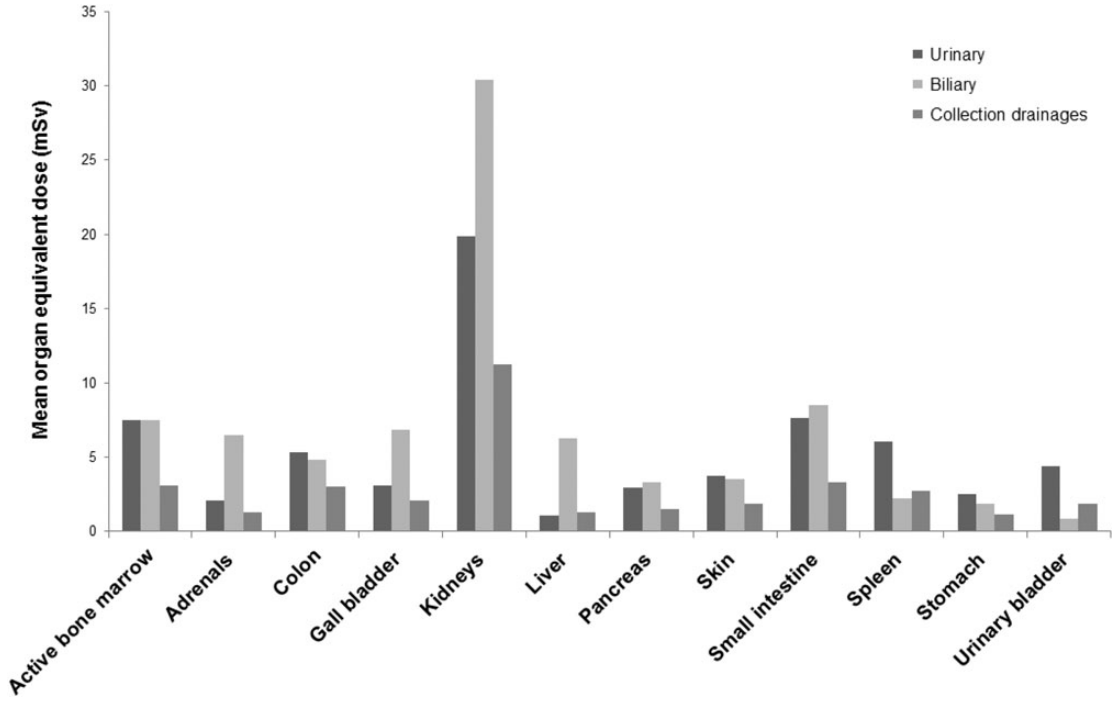

Figure 3. Histogram of mean organ equivalent doses per kind of intervention.

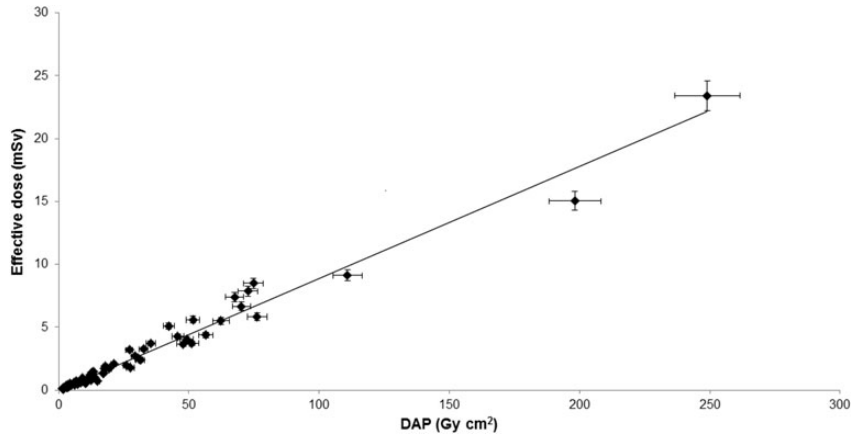

Figure 4. Relationship between effective dose and DAP values.

simulation the real energy beam spectra, the real geometric projection and distances, the actual organs (or part of them) covered by the irradiation field of each procedure.

CONCLUSION

The presented method that automatically extracts DICOM information, complemented by the Monte Carlo simulator PCXMC, is a feasible and promising approach for easily monitoring patient dose and optimising the IR procedures in order to limit the risk of stochastic and deterministic effects. The presented method allows to customise the dose calculation, in order to produce a dosimetric report for each patient; this report could be fundamental, especially for patients undergoing repeated X-rays procedures. Finally, knowledge and

easy calculation of the equivalent doses related to each interventions contribute to collect patient-specific dosimetric information and to evaluate associated risks to X-ray exposure according to the type of procedure.

REFERENCES

1. Dendy, P. P. *Radiation risks in interventional radiology.* Br. J. Radiol., **81**, 1–7 (2008).
2. Stecker, M. S. *et al. SIR Safety and Health Committee, CIRSE Standards of Practice Committee. Guidelines for patient radiation dose management*. J. Vasc. Interv. Radiol., **20**(7 Suppl), S263–S273 (2009).
3. Panzer, W., Petoussi, N. and Zankl, M. *Effective dose—how effective for patients?* Radiat. Environ. Biophys., **32**, 209–219 (1993).
4. Kemerink, G. J., Kicken, P. J. H., Schultz, F. W., Zoeteliefand, J. and Van Engelshoven, J. M. A. *Patient dosimetry in abdominal arteriography.* Phys. Med. Biol., **44**, 1133–1145 (1999).
5. Miller, D. L. *et al. Radiation doses in interventional radiology procedures: the RAD-IR study: part II: skin dose.* J. Vasc. Interv. Radiol., **14**, 977–990 (2003).
6. Rampado, O. and Ropolo, R. *A method for a real time estimation of entrance skin dose distribution in interventional neuroradiology.* Med. Phys., **31**, 2356–2361 (2004).
7. D'Alessio, D., Giliberti, C., Soriani, A., Carpanese, L., Pizzi, G., Vallati, G. E. and Strigari, L. *Dose evaluation for skin and organ in hepatocellular carcinoma during angiographic procedure.* J. Exp. Clin. Canc. Res., **32**, 81 (2013).
8. Kloeckner, R., Bersch, A., Dos Santos, D. P., Schneider, J., Duber, C. and Pitton, M. B. *Radiation exposure in nonvascular fluoroscopy-guided interventional procedures.* Cardiovasc. Intervent. Radiol., **35**, 613–620 (2012).
9. Karavasilis, E., Dimitriadis, A., Gonis, H., Pappas, P., Georgiou, E. and Yakoumakis, E. *Effective dose in percutaneous transhepatic biliary drainage examination using PCXMC2.0 and MCNP5 Monte Carlo codes.* Phys. Medica, **30**, 432–436 (2013).
10. Stratakis, J., Damilakis, J., Hatzidakis, A., Perisinakis, K. and Gourtsoyiannis, N. *Radiation dose and risk from fluoroscopically guided percutaneous transhepatic biliary procedures.* J. Vasc. Interv. Radiol., **17**, 77–84 (2006).
11. Jones, A. K. and Pasciak, A. S. *Calculating the peak skin dose resulting from fluoroscopically guided interventions. Part I: methods.* J. Appl. Clin. Med. Phys., **12**, 231–244 (2011).
12. *Early and Late Effects of Radiation in Normal 16 Tissues and Organs: Threshold Doses for Tissue 17 Reactions and Other Non-Cancer Effects of 18 Radiation in a Radiation Protection Context*. Annals of the ICRP. ICRP ref 4844–6029–7736 (2011).
13. *European Guidance on Estimating Population Doses from Medical X-Ray Procedures.* European Commission Radiation Protection N. 154 (2008).
14. *Establishing Guidance Levels in X-Ray Guided Medical Interventional Procedures: A Pilot Study.* Safety Reports Series n. 59, IAEA (2009).
15. Hart, D., Hillier, M. C. and Wall, B. F. *National reference doses for common radiographic, fluoroscopic and dental X-ray examinations in the UK.* Br. J. Radiol., **82**, 1–12 (2009).
16. Wielandts, J. Y., Smans, K., Ector, J., De Buck, S., Heidbuchel, H. and Bosmans, H. *Effective dose analysis of three-dimensional rotational angiography during catheter ablation procedures.* Phys. Med. Biol., **55**, 563–579 (2010).